

# Effects of Multi-directional Shaking in Nonlinear Site Response Analysis: Case Study of 2007 Niigata-ken Chuetsu-oki Earthquake

R. Motamed<sup>1</sup>, K.V. Stanton<sup>2</sup>, I. Almufti<sup>3</sup>, K. Ellison<sup>4</sup>, M. Willford<sup>5</sup>

## ABSTRACT

Nonlinear ground response analyses are conducted for the 2007 Niigata-ken Chuetsu-oki earthquake recorded at a free-field vertical array near the Kashiwazaki-Kariwa Nuclear Power Plant in Japan. A soil column is built in LS-DYNA using three-dimensional elements which allow for multi-directional shaking analyses as well as user-defined stress-strain relationships to dictate soil behavior under dynamic loading. Dynamic soil behavior is characterized using a two-stage hyperbolic backbone curve implemented with modifications to consider not only the peak strength of soil layers but also the strain at which it is fully mobilized. Input bedrock motions are applied in the following directions: one-directional Fault Normal (FN), one-directional Fault Parallel (FP) and two-directional FN and FP. To better understand the effects of modeling two-directional shaking, analyses are conducted with input motions scaled to 50%, 100% and 150%. The results suggest that a two-directional analysis has the potential to provide more accurate site response estimates, especially for stronger ground motions.

## Introduction

The effects of multi-directional shaking are not typically considered in conventional site response analyses. However, a true representation of the physical process in which seismic energy propagates to the ground surface would consider all directions wave energy could potentially dissipate (i.e. a three-directional analysis). Thus, in an effort to maintain a practical level of complexity while maximizing model accuracy, a site response analysis which considers two-directional (2D) input shaking was conducted and is presented herein. The results of this analysis are also compared to that of a one-directional (1D) counterpart to evaluate the impact of including two horizontal shaking components.

Past research suggests that 2D site response analyses may be worthwhile. Stewart et al. (2008) used the finite element software OpenSees (Mazzoni et al., 2009) to show that, in part, wave energy can be diverted from the direction of stronger to weaker input shaking if motion is allowed to occur in two directions simultaneously. In addition, Bolisetti et al. (2014) used LS-DYNA (LSTC, 2012) to show that the predicted response from a 1D analysis of a hypothetical soil column differed more greatly from that of a 2D analysis as the intensity of input shaking increased. A 2D analysis from Motamed et al. (2015) gave predictions which matched measured response data more closely than that from a 1D analysis of the same site. These analyses were conducted using only a single set of input motions which were measured at a free-field downhole

---

<sup>1</sup>Asst. Professor, Dep. Civil & Env. Eng., University of Nevada, Reno, USA. [motamed@unr.edu](mailto:motamed@unr.edu)

<sup>2</sup>Graduate Student, Dep. Civil & Env. Eng., University of Nevada, Reno, USA. [kevinstanton@nevada.unr.edu](mailto:kevinstanton@nevada.unr.edu)

<sup>3</sup>Associate, Arup, San Francisco, CA, USA.

<sup>4</sup>Senior Engineer, Arup, San Francisco, CA, USA.

<sup>5</sup>Principal, Arup, San Francisco, CA, USA.

array, known as the Service Hall Array (SHA), near the Kashiwazaki-Kariwa Nuclear Power Plant in Japan. The study also investigated new methods for characterizing dynamic soil behavior using a two-stage hyperbolic backbone curve with fitting parameters which allow large strain response to be fit to empirically derived response from Hayashi et al. (1994) for cohesionless material and Vardanega et al. (2012) for cohesive material. Thus, to improve our understanding of conditions for which 2D site response analyses are most appropriate, the methods from Motamed et al. (2015) are carried out herein for the same input motions scaled to 50%, 100% and 150% of their original content.

The finite element program LS-DYNA was employed for the analyses in this study. Dynamic soil behavior was represented using the MAT\_HYSTERETIC\_SOIL model available within LS-DYNA. This allowed the dynamic properties to be characterized with user-defined stress-strain inputs for each soil layer and enabled corrections for the effects of strain rate which were applied in accordance with the recommendations of Vardanega and Bolton (2013). Hence, for cohesive soil layers only, stiffness was increased by 5% per log cycle of shear strain rate. Due to the nonlinear nature of soil, shear stresses in the principal directions are typically correlated (Hadjian, 1981). Therefore, the assumptions inherent to a 1D site response analysis may not be valid. The MAT\_HYSTERETIC\_SOIL model accounts for the relationship between mobilized stresses in different directions by defining the yield surface of each layer in terms of the stress invariant  $J_2$ , which is determined internally based on the prescribed maximum shear stress associated with a uniaxial stress state. This allows for a correlated response in orthogonal directions but requires a unique stress-strain model to be defined for each independent layer of the soil profile.

### Site Characterization

The soil conditions at the SHA were assumed based on site data provided by the Tokyo Electric Power Company (TEPCO) as well as shear wave velocity and laboratory testing data from Yee et al. (2013). Figure 1 shows the geologic section, location of sensors and assumed velocity profile of the site. Additional information regarding the site characterization is given in Yee et al. (2013).

A summary of the assumed soil types and unit weights is given in Table 1. It should be noted that, based on data from TEPCO, the ground water table was modeled at 45.5m depth.

Table 1. Assumed soil types and unit weights used for analysis.

Depth Range (m)	Soil Type	Unit Weight (kN/m <sup>3</sup> )
0 - 4	Sand	16
4 - 45	Sand	17.75
45 - 70	Sand	20.8
70 - 99.4	Clay	20.8

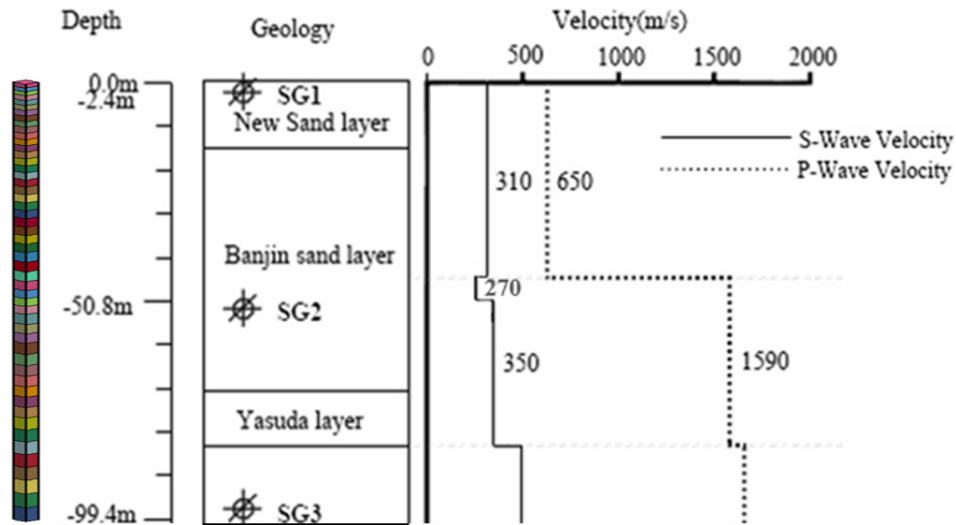


Figure 1. LS-DYNA soil column, geologic section, location of sensors,  $V_s$  and  $V_p$  logging data at the SHA (modified from original figure provided by TEPCO)

### LS-DYNA Model and Dynamic Soil Properties

The LS-DYNA model was built using vertically stacked solid three-dimensional elements which were constrained to move in shear and allowed the soil to be subjected to multi-directional shaking. In LS-DYNA, the response of soil layers was calculated by solving the dynamic equations of motions with the explicit method. Dynamic soil properties were defined such that nonlinear shear stiffness was accounted for in a piecewise manner by separating the shear behavior across multiple linear elastic-perfectly plastic yield surfaces. Also, the backbone curve of the shear stress-strain at a reference pressure was used to control the elastic stiffnesses and sizes of the yield surfaces. Modulus degradation and damping were determined internally based on user defined stress-strain inputs and the effects of strain rate in cohesive layers were incorporated through a viscoplastic formulation that automatically adjusted the sizes of the yield surfaces.

The backbone curve for each of the soil layers in the model was defined using a two-stage formulation given in Equations 1 and 2.

$$\frac{G}{G_{\max}} = \frac{1}{1 + \beta \left( \frac{\gamma}{\gamma_r} \right)^\alpha} \quad (1) \quad \frac{G}{G_{\max}} = \frac{1}{1 + \beta (\gamma/\gamma_r)^\alpha}$$

$$\frac{G}{G_{\max}} = \frac{\frac{\gamma_1}{1 + \beta \left( \frac{\gamma}{\gamma_r} \right)^\alpha} + \frac{\left( \frac{G_{\gamma_1}}{G_{\max}} \right) \gamma'}{1 + \beta' \left( \frac{\gamma'}{\gamma_{ref}} \right)^\alpha}}{\gamma} \quad (2)$$

Where  $\gamma_1$  is the transition strain,  $\alpha$ ,  $\alpha'$ ,  $\beta$  and  $\beta'$  are curve fitting parameters and  $\gamma_r$  is the pseudo-reference strain (the strain at which the normalized shear modulus is 0.5).

Using the above functional form, the shear stress-strain curves were defined using a similar method as in Motamed et al. (2015). The primary difference between the approach herein and Motamed et al. (2015) is associated with the transition strains chosen for each layer. In this study, the transition strains, which are discussed in greater detail in Motamed et al. (2015) and Yee et al. (2013), were chosen on a layer-by-layer basis such that abrupt changes in the slopes of the modulus degradation, damping and shear stress-strain curves were minimized.

The curve fitting parameters  $\alpha$  and  $\beta$  were taken from Yee et al. (2013) while  $\alpha'$  and  $\beta'$  were determined using an algorithm, implemented with Excel Visual Basic for Applications (VBA), which produced a smooth curve fit to target stress-strain data at large strains (i.e. strains greater than the transition strain). The target stress-strain values were assigned with the approach from Motamed et al. (2015) and rely on relationships given in Hayashi et al. (1994) for sand and Vardanega and Bolton (2013) for clay. Overall,  $\alpha'$  and  $\beta'$  both ranged between 0.95 and 1.05 and  $\gamma_1$  ranged between 0.07 and 0.14%.

The soil column was discretized into 51 layers such that the maximum frequency each layer could propagate was as close to 37.5 Hz as possible. This value was chosen based on the average of recommendations given in Kwok et al. (2007). In addition, small strain damping of 2% was applied using the DAMPING\_FREQUENCY\_RANGE\_DEFORM option in LS-DYNA which adds frequency independent damping to a prescribed frequency range outside of which the additional damping gradually decreases to zero. According to the LSTC (2012), the bounds of the frequency range should not differ by more than a factor of 30 and in this study were set to 3.33 Hz and 100 Hz. The value chosen for small strain damping was based on the approximate average of values calculated for all layers using the method given in Darendeli (2001).

## Results

The input ground motions used to develop the results were recorded at the SHA at a depth of 99.4m during the 2007 Niigata-ken Chuetsu-oki earthquake ( $M_w=6.6$ ) and scaled to 50%, 100% and 150%. For each scaled input, 1D fault normal (FN), 1D fault parallel (FP) and 2D FN-FP analyses were conducted. Similar to other site response analysis studies involving LS-DYNA, such as Motamed et al. (2015) and Bolisetti et al. (2014), high frequency “numerical noise” was initially present in the results. While this noise appears to be minimal herein compared past studies with LS-DYNA, perhaps due to the stricter layer discretization discussed in the last section, a low-pass Butterworth filter with a cutoff frequency of 35 Hz was still applied to correct the computed acceleration data. The results are presented in Figures 2 through 6.

Figure 2 shows the response spectra at different depths and input motion intensities. From this, compared to the generally similar match to the 2D prediction for the 50% scaled input motion, the 1D predictions become more different from that of the 2D as the input motion is scaled up.

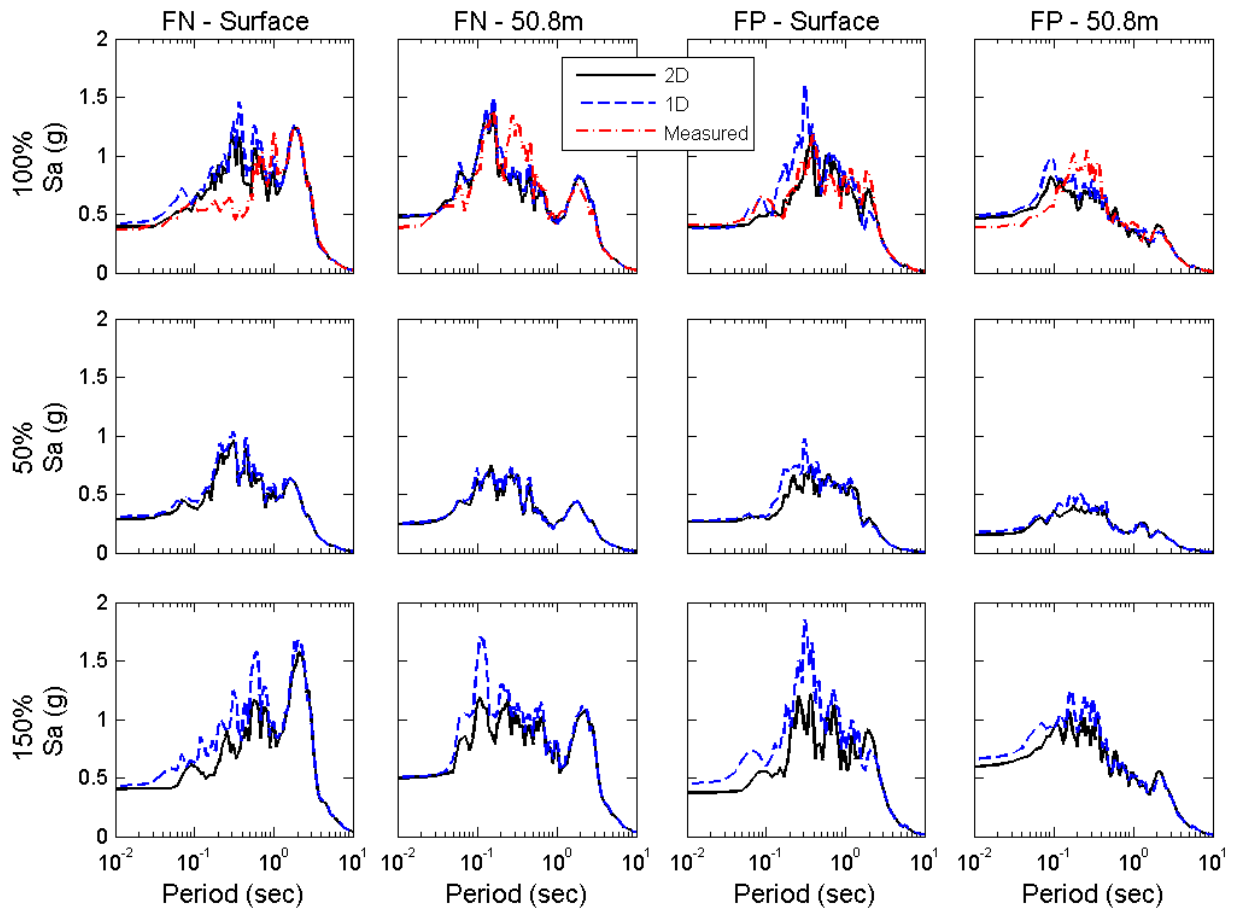


Figure 2. Response spectra for both 1D and 2D input motions scaled to 50%, 100% and 150%

Figures 3 and 4 depict the error associated with the computed response and comparability of the 1D and 2D predictions, respectively. In general, Figure 3 suggests that the 2D predictions match the measured response spectra more closely than that of the 1D analyses. This difference is more noticeable at the ground surface than at the 50.8m depth for the unscaled results but Figures 2 and 4 reveal that when the input motions are scaled to 150%, the computed 1D responses deviate further from the 2D computed values at both levels. Additional inspection of Figure 2 shows that the 1D analyses tend to be sensitive to increased ground shaking in the period range of approximately 0.2 to 0.6 seconds.

The computed strain profiles from Figure 5 show much less dependence on multi-directional input shaking than the response spectra results. Except for some small differences in the computed responses at 150% scaling, all of the strain profiles are essentially the same. In contrast, the PGA profiles from Figure 6 show a slightly greater impact of 1D versus 2D modeling, especially as the input motions are increased. It is interesting to note that at 150% ground shaking, the 1D PGA results are consistently greater than the 2D results. This trend is also reflected in the response spectra from Figure 2.

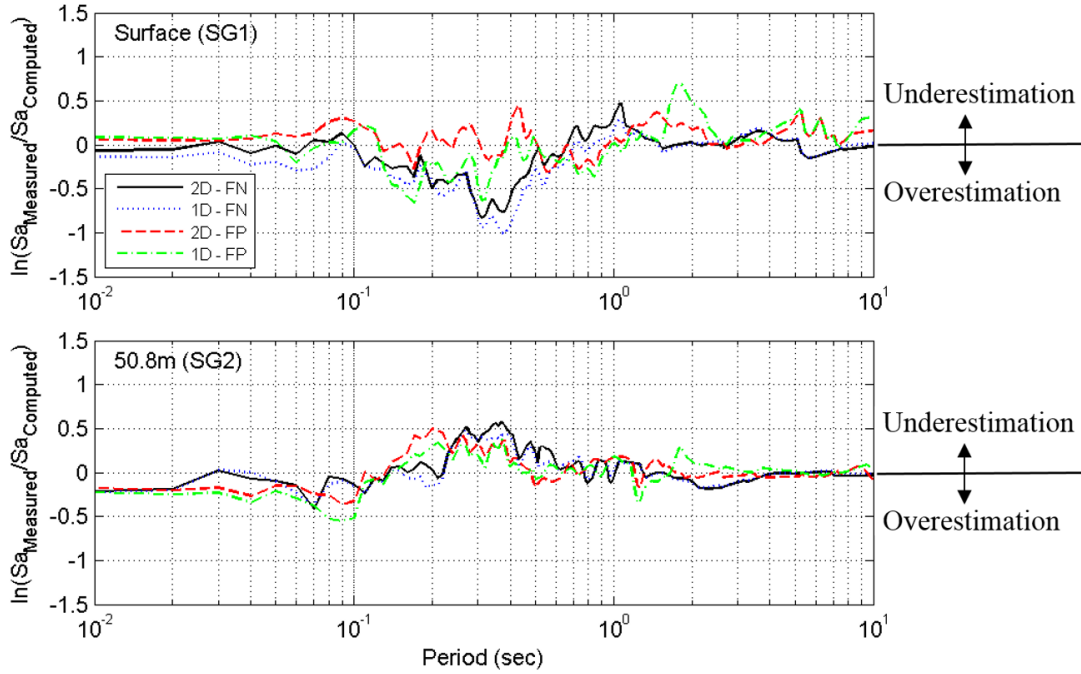


Figure 3. Natural logarithm of the ratio between the measured and computed spectral accelerations for the FN and FP components at the surface and a depth of 50.8m

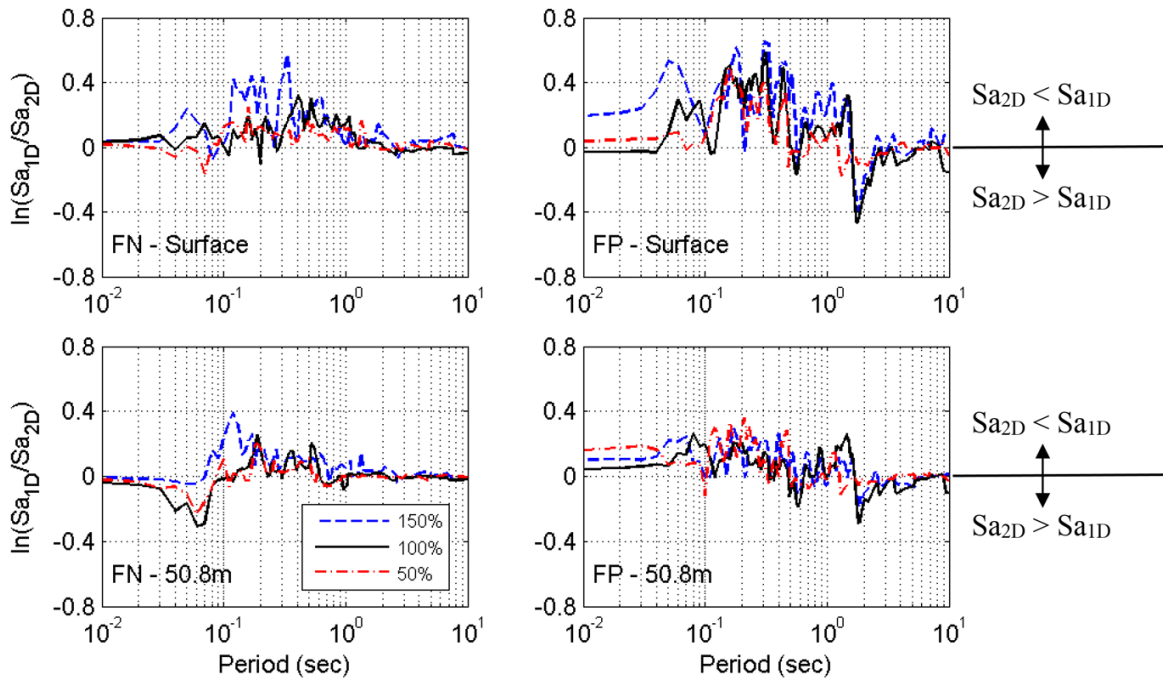


Figure 4. Natural logarithm of the ratios between the 1D and 2D computed spectral accelerations for 50%, 100% and 150% of the original input motions

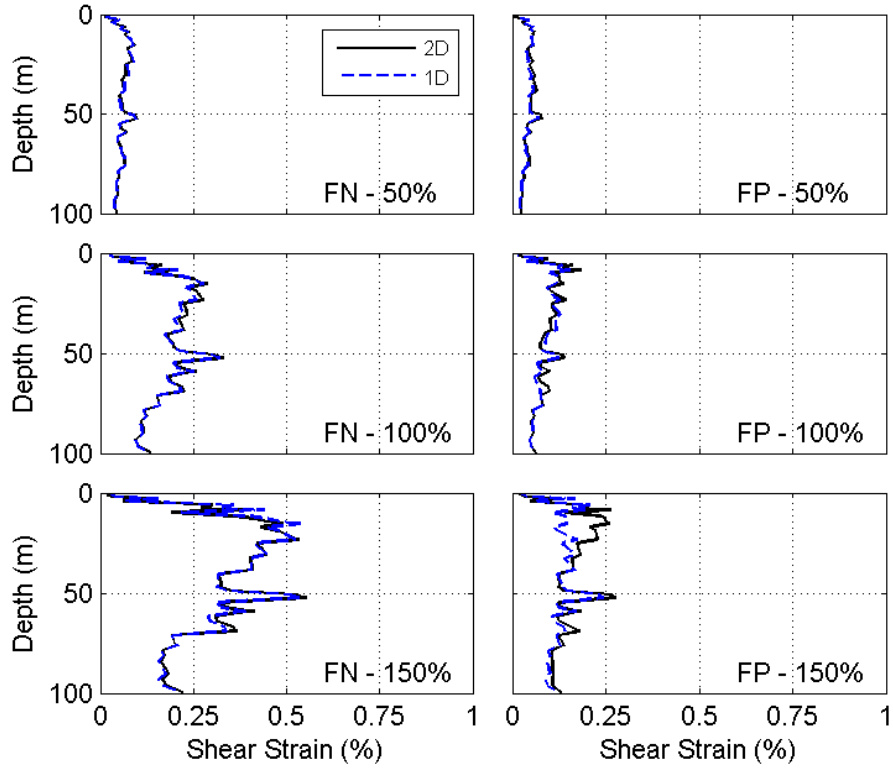


Figure 5. Strain profiles computed using 1D and 2D input motions scaled to 50%, 100% and 150%

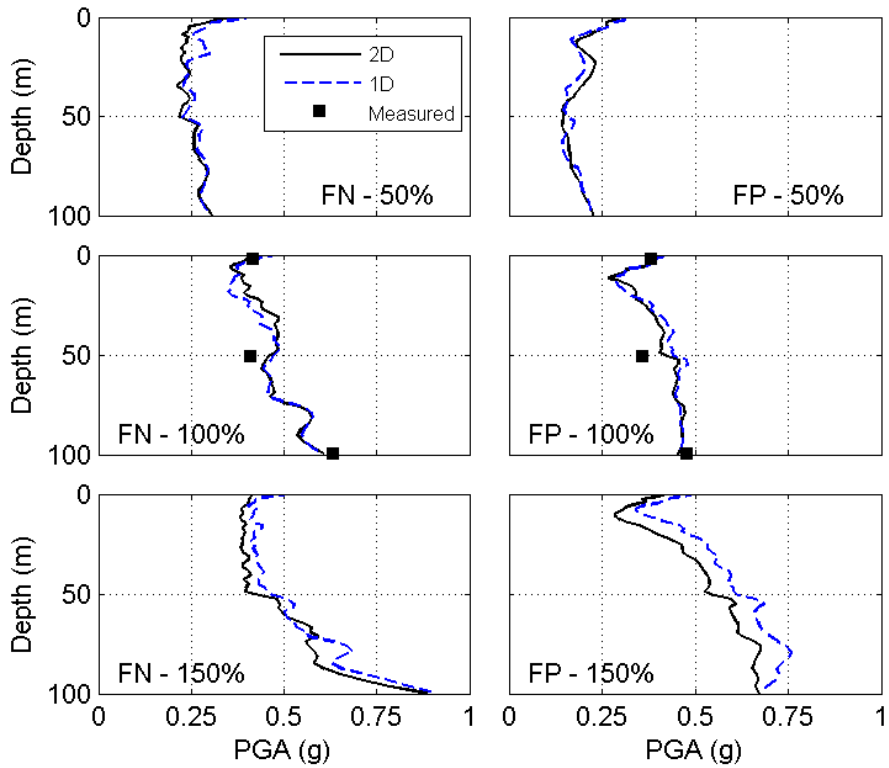


Figure 6. PGA profiles computed using 1D and 2D input motions scaled to 50%, 100% and 150%

## Conclusions

The results suggest that as the magnitude of input motions increases, the differences between the 1D and 2D results become generally more pronounced. That being said, little to no differences are evident when comparing the results for the input motions scaled to 50% and only some cases at 100% input shaking show significant dissimilarities. For the 150% scaled input, however, the PGA, strain and spectral response data were less comparable for the 1D and 2D analyses. Thus, based on these observations, it seems that a 2D analysis provides a significant advantage when the peak spectral acceleration is in excess of about 1g.

In general, the 1D analyses appear more prone to overestimation of spectral response and PGA than underestimation. Conversely, the strain results herein suggest that a 1D analysis may predict either higher or lower strains than a 2D analysis, though it seems that strain is far less sensitive to the dimensions of the model.

It is important to note that the conclusions drawn in this study are only pertinent to the SHA and other sites associated with similar soil types, nonlinearity in measured response and any other factors which may influence the tendency for energy to shift from one direction to another. That being said, however, it is unreasonable to assume that the findings of this study represent a unique phenomenon. Thus, based on the results of this study, it is important to consider the effects of multi-directional input shaking in site response analyses until our understanding of when a 1D analysis acceptable is significantly improved. The results also suggest that this is especially true for sites which have large recorded ground motions.

## Acknowledgments

We would like to thank Dr. Yuli Huang and Dr. Jongwon Lee of Arup for the useful discussions and valuable comments they provided. We would like to acknowledge that the ground motion data used in this study belongs Tokyo Electric Power Company, and the distribution license of the data belongs to Japan Association for Earthquake Engineering.

## References

- Bolisetti, C., Whittaker, A. S., Mason, H. B., Almufti, I., & Willford, M. (2014). Equivalent linear and nonlinear site response analysis for design and risk assessment of safety-related nuclear structures. *Nuclear Engineering and Design*, **275**: 107-121.
- Darendeli, M. (2001). *Development of a new family of normalized modulus reduction and material damping curves*. Ph.D. Dissertation, University of Texas, Austin, Department of Civil Engineering.
- Hadjian, A.H., 1981. On the correlation of the components of strong ground motion– Part 2. *Bulletin of the Seismological Society of America*, **71**(4): 1323–1331.
- Hayashi, H., Honda, M., Yamada, T., & Tatsuoka, F. (1994). Modeling of nonlinear stress-strain relations of sands for dynamic response analysis. *Earthquake Engineering, Tenth World Conference*, (pp. 6819-6825). Balkema, Rotterdam.
- Kwok, A. O., Stewart, J. P., Hashash, Y. M., Matasovic, N., Pyke, R., Wang, Z., & Yang, Z. (2007). Use of exact solutions of wave propagation problems to guide implementation of nonlinear seismic ground response analysis procedures. *Journal of Geotechnical and Geoenvironmental Engineering*, **133**(11): 1385-1398.



LSTC, 2012. LS DYNA Keyword User's Manual Volumes I & II – Release 971 R6.1.0. Livermore Software Technology Corporation, Livermore, California.

Mazzoni, S., McKenna, F., Scott, M.H., Fenves, G.L., 2009. Computer Program OpenSees: Open System for Earthquake Engineering Simulation. Pacific Earthquake Engineering Research Center (PEER), University of California, Berkeley, California.

Motamed, R., Stanton, K.V., Almufti, I., Ellison, K., and Willford, M. (2015). Improved Approach for Modeling Nonlinear Site Response of Highly Strained Soils: Case History of the Service Hall Array in Japan. *Earthquake Spectra* (currently under review).

Stewart, J.P., Kwok, A.O., Hashash, Y., Matasovic, N., Pyke, R., Wang, Z., and Yang, Z. (2008). *Benchmarking of Nonlinear Ground Response Analysis Procedures*. PEER Report 2008/04, Pacific Earthquake Engineering Research Center, University of California at Berkeley, August, 205 pp.

Vardanega, P. and Bolton, M. (2013). Stiffness of Clays and Silts: Normalizing Shear Modulus and Shear Strain. *Journal of Geotechnical and Geoenvironmental Engineering*, **139**(9): 1575–1589.

Vardanega, P., Lau, B., Lam, S., Haigh, S., Madabhushi, S., & Bolton, M. (2012). Laboratory Measurement of Strength Mobilisation in Kaolin: Link to Stress History. *Geotechnique Letters*, **2**(1): 9–15.

Yee, E., Stewart, J. P., & Tokimatsu, K. (2013). Elastic and Large-Strain Nonlinear Seismic Site Response Analysis of Vertical Array Recordings. *Journal of Geotechnical and Geoenvironmental Engineering*, **139**: 1789-1801.